

Large Deformations during the Coalescence of Fluid Interfaces

Nianhuan Chen, Tonya Kuhl,* Rafael Tadmor,[†] Qi Lin, and Jacob Israelachvili[‡]

*Department of Chemical Engineering, Materials Department, Materials Research Laboratory,
and the Biomolecular Science and Engineering Program, University of California, Santa Barbara, California 93106, USA*

(Received 15 May 2003; published 15 January 2004)

Surface forces and shape changes were simultaneously measured during the approach and coalescence of two liquid-liquid and liquid-air interfaces. Large normal and lateral deformations were observed that are nevertheless consistent with a simple theoretical analysis of the long-range effects of short-range attractive van der Waals forces. The results imply that two fluidlike structures such as liquid droplets and soft biological cells can sense each other at much larger separations than previously assumed based on criteria taken from the interactions of hard particles.

DOI: 10.1103/PhysRevLett.92.024501

PACS numbers: 47.20.Ma

Droplet or liquid-liquid coalescence is important for understanding emulsion stability, capillary condensation, cloud formation, and many biological processes such as cell-cell interactions [1–3]. However, the mechanisms of coalescence are still not well understood, especially at the molecular-level where intersurface forces act together with surface tension and viscous forces. There have been no reports of how coalescence occurs at the nanoscale or the way molecular forces are involved in the deformations leading to coalescence. Theories of coalescence have been mainly based on continuum hydrodynamic forces or scaling theories [4,5] which have difficulties in incorporating molecular-level interactions.

Attractive molecular forces result in the adhesion or coalescence of two approaching liquid surfaces or interfaces unless the opposing viscous forces are too large. Three distinct coalescence regimes or processes can be distinguished that depend on the rate of approach relative to the characteristic interaction time [6]. First, the interaction can occur at constant liquid volume, which is a common supposition. Examples of *mechanical* instabilities include the Rayleigh instability [7] of a nonspherical droplet due to surface tension forces or the deformations and coalescence of two droplets due to the van der Waals (VDW) force between them. Second, coalescence can occur as a *critical* instability, akin to a nucleation process, which is triggered by a large thermal fluctuation. Finally, coalescence can occur at true *thermodynamic* equilibrium, when the chemical potential of the liquid molecules are in equilibrium with the vapor or solvent reservoir at all times. Under these conditions the volume of the two coalescing liquids changes as their surfaces approach each other due to the condensation of molecules from the vapor phase [8–10]. Thermodynamic instabilities are sensitive to the vapor pressure.

Here we report the results of experiments where two supported involatile liquid layers were made to approach each other in vapor or immersed in another liquid medium. Simultaneously, the deformations and forces between the surfaces were measured, and any coalescence

was visualized in real time by employing multiple beam interference fringes.

A surface forces apparatus (SFA Mark III) was used to measure the forces between and the changing shapes of two surfaces [cf. Figures 1(a) and 1(b)] [12]. The distance between the two surfaces D and the film thickness T was determined optically from simultaneous measurements of adjacent fringes of equal chromatic order (FECO) in the spectrogram, and solving for D and T using a modified version of the basic equation for a symmetrical five-layer interferometer [13] in which the refractive indices of the three media are known. The nonpolar liquid PDMS and the nonpolar polymer PBD were used as the interacting or intervening fluids. PBD and PDMS are immiscible and involatile, which make them particularly suitable for these studies.

The PBD or PDMS layers on the mica substrates were deposited either by retracting the substrates from the pure liquid or a solution in toluene, solvent cast from toluene, or spin coated, to produce smooth uniformly thick layers of thickness $T_0 = 4\text{--}350$ nm, as ascertained from the FECO fringes which had a height (film roughness) resolution of 1 nm and a lateral (waviness) resolution of 1 μm . The surfaces were then placed in the SFA to face each other in the crossed cylinder configuration. Each cylinder was of radius $R \sim 1\text{--}2$ cm. The surfaces were brought towards each other at different driving velocities V ranging from 0.01 to 50 nm/s while measuring the force F between them as a function of the surface separation D and the film thickness T from the changing wavelength positions and shapes of the FECO fringes. Experiments were performed either in vapor (dry nitrogen gas) or with PBD or PDMS films totally immersed in PDMS or PBD. To measure the forces, one of the surfaces was mounted at the end of a double-cantilever “force-measuring” spring of stiffness $K \approx 10^3$ N/m. In some cases, when only the film profiles were measured, the surfaces were mounted on rigid supports, effectively on springs of infinite stiffness.

The theoretically expected van der Waals force between the two curved liquid or solid surfaces is $F = -AR/6D^2$,

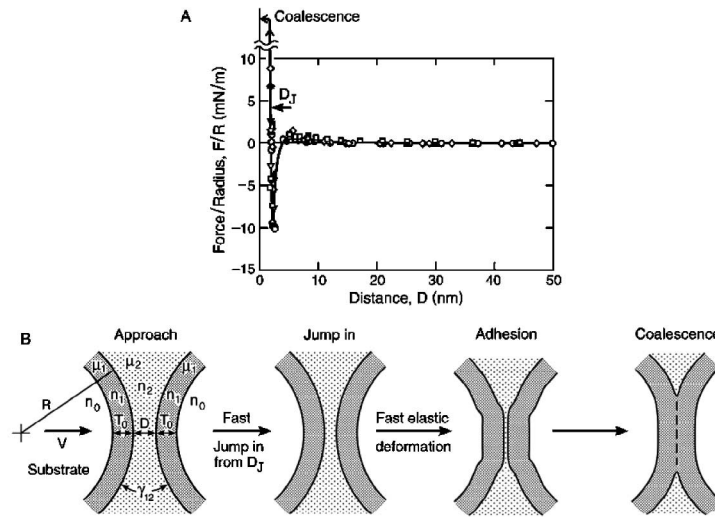


FIG. 1. (a) Measured force-distance function $F(D)$ between two hard, solidlike polybutadiene (PBD) layers (medium 1) of molecular weight $\sim 10^6$ Da and thickness $T_0 = 110$ nm immersed in liquid polydimethyl-siloxane (PDMS) (medium 2, $\mu_2 = 0.0015$ Pa \cdot s). The measured forces were independent of the approach velocity V in the range from 0.01 to 50 nm/s. (b) Surface geometry relevant to this work where all measurements were done at 25 $^\circ$ C. In the case of the solidlike PBD layers whose interaction in PDMS is described in (a), a monolayer or two of PDMS are transiently trapped between the two PBD surfaces immediately after they jump into adhesive “contact” due to the short-range structural forces previously observed both in PBD and PDMS. The crossed-cylinder geometry used in these SFA experiments is locally equivalent, to first order, to two spheres having twice the radius of the cylinders (Ref. [11], Chap. 11). The simplified schematic profiles shown in this and subsequent figures are drawn for convenience.

where A is the Hamaker constant which, based on the Lifshitz theory [Ref. [11], Eq. (11.14)], is estimated to be $A = 5 \times 10^{-20}$ J for two PDMS surfaces interacting in air, and $A = 6.6 \times 10^{-21}$ J for two PBD surfaces interacting across PDMS.

Figure 1(a) shows the “quasistatic” forces measured between two solidlike PBD films in liquid PDMS where only attractive VDW forces are expected. The measured jump-in distance of $D_J \sim 4$ nm is in agreement with the theoretically expected distance based on the criterion for a jump instability [14]: $dF/dD = AR/3D_J^3 = K$, viz.,

$$D_J = (AR/3K)^{1/3}, \quad (1)$$

where, in this case, inserting $A = 6.6 \times 10^{-21}$ J, $R = 1.0$ cm, and $K \approx 3.7 \times 10^3$ N/m gives $D_J = 4$ nm. The separation at the jump is also surprisingly close to that estimated from droplet coalescence experiments using the four-roll mill technique [15]. No deformations of the surfaces or any change in the thickness of the films were detected prior to the jumps into contact.

Figure 2 shows the changing shapes of two fluid surfaces interacting across air or a fluid film, as well as some typical FEKO images visualized at various stages on approach and coalescence. Those FEKO images most clearly show some of the more interesting features shown in the schematics below them. Unlike the much simpler coalescence mechanism described in Fig. 1, the details now depend on many additional factors, including the initial layer thickness T_0 , the viscosities of the two liquids μ_1 and μ_2 , their interfacial tension γ_i , and especially the

approach rate V . In addition, short-range (< 2 nm) structural forces [11,16] were again evident in these systems [cf. Fig. 1(b)] where adhesive contact was not immediately followed by coalescence. The interactions shown in Fig. 2 will be described in detail elsewhere.

Figure 3 shows detailed measurements of the changing film and gap thicknesses T and D when [Fig. 3(a)] two surfaces of liquid PDMS approach each other in air, and when [Figs. 3(b) and 3(c)] two surfaces of liquid PBD approach each other in PDMS. In the case of Fig. 3(a), presumably because of the absence of an intervening viscous medium, a mechanical instability occurred where the two liquid layers suddenly thickened, “jumped” into contact, and coalesced.

Figures 3(b) and 3(c) show the changing film and gap thicknesses of two liquid PBD films approaching each other in liquid PDMS. Because of the viscous medium between the two PBD surfaces, the coalescence is more sluggish than in air, and the bulging is more pronounced for smaller V and thicker films T_0 (cf. the much larger bulging in Fig. 3(b) than in Fig. 3(c) where the PBD film was 5 times thinner). Other deformations are also evident in these systems both preceding and following the jumps into contact. These will be described elsewhere.

Forcada *et al.* [17] were the first to theoretically analyze the thickening of a liquid film on a substrate surface due to its interaction with an atomic force microscope tip. A number of recent theoretical publications have addressed the issue of liquid-liquid coalescence in terms of the “effective stiffness” of a liquid surface or interface

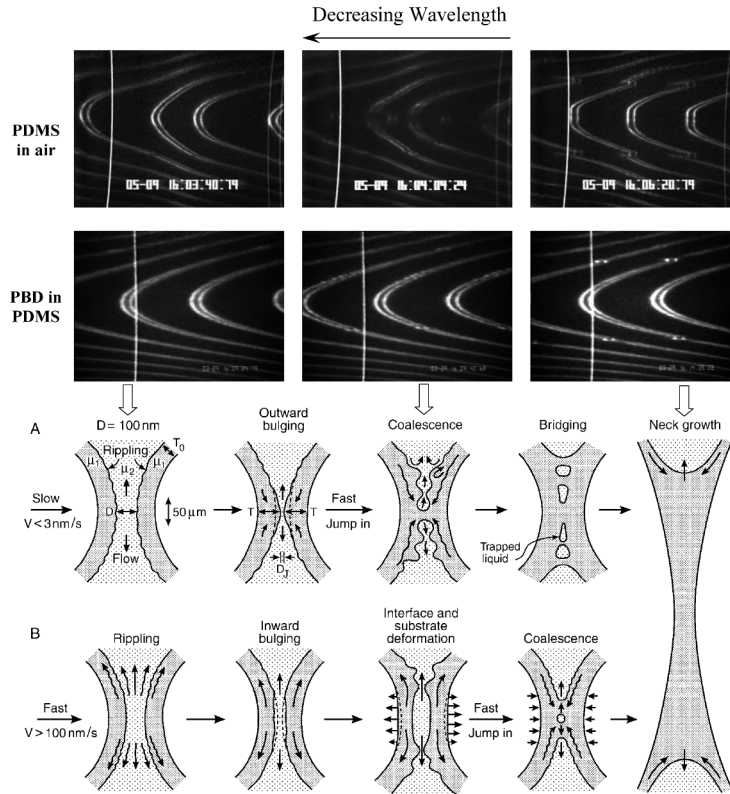


FIG. 2. Visualized FECO images (top two rows) and corresponding schematics (bottom two rows) of changing surface profiles of two liquid films on approach and coalescence. Top row: FECO images of two PDMS liquid films approaching and coalescing in air. Second row: FECO images of two PBD liquid films approaching and coalescing in liquid PDMS. The shapes and wavelength positions of the FECO fringes give information on the thicknesses of and separation between the two liquid films [13]. The bottom two rows show schematic profiles of two liquid PBD films approaching each other in liquid PDMS on (a) slow and (b) fast approach velocities V , as deduced from an analysis of the changing FECO fringe patterns (cf. second row) with time. Depending on the experimental conditions, especially T_0 , μ_i , and V , micron-wavelength ripples were often observed off center both before and after coalescence.

[18–21] and have concluded that a liquid surface behaves like a Hookian spring with an effective stiffness K_{eff} equal to its surface or interfacial tension, viz.,

$$K_{\text{eff}} \approx \gamma \quad \text{or} \quad \gamma_i. \quad (2)$$

Thus, K_{eff} replaces K in Eq. (1) for the jump or instability distance D_J . For PDMS in air we therefore expect an effective stiffness of 0.030 N/m, while for the PBD/PDMS interface we expect a stiffness of 0.004 N/m. These are extremely low values when compared to those of order 10^2 – 10^4 N/m that are commonly employed in surface force measurements. But more importantly they suggest (i) that liquid surfaces become highly distorted even by the smallest force (either attractive or repulsive) and (ii) that jump distances into adhesive contact or coalescence are likely to be very large. For example, for a surface of liquid PDMS in air the jump distance in a SFA experiment is expected to be given by Eq. (1) as $D_J = (AR/3K_{\text{eff}})^{1/3} = [(5 \times 10^{-20})(0.02)/(3 \times 0.030)]^{1/3} \approx 220$ nm, and similarly large distances are predicted for PBD in PDMS (since both A and K_{eff} are reduced by similar amounts). The above calculation is an overestimate because it ignores retardation effects [11].

However, the measured jumps of order ~ 200 nm shown in Fig. 3 are in good agreement with the theoretical estimates calculated above. (iii) We may also note that the lateral (in-plane) deformations are much greater than the normal (out-of-plane) bulging, which is as expected for liquid-vapor and liquid-liquid interfaces [17,22]. However, the effective stiffness K of such interfaces is expected to be only weakly dependent on the exact geometry of the bulge and so does not require macroscopic surface deformations; i.e., *local* bulging should result in large, qualitatively similar, instabilities.

Since according to Eq. (1) D_J scales as $R^{1/3}$, our results would imply smaller but still very significant deformations for small droplets or biological cells. For example, for droplet diameters in the range 1–10 μm , deformations of order 10–20 nm are expected. Thus, two liquid droplets or fluidlike biological cells will start to interact with each other at separations that are much larger than between rigid colloidal particles. These “action-at-a-large-distance” effects have important consequences for our understanding of the effective range of molecular forces between soft particles, and how they attract, repel, deform, and coalesce. In the above example the

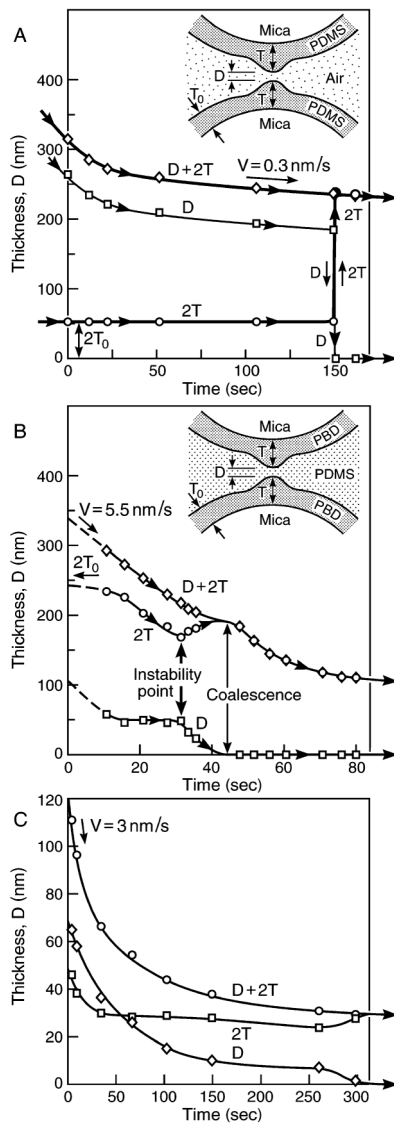


FIG. 3. (a) Changing thickness of liquid films of PDMS (molecular weight ~ 45 kDa; viscosity $\mu_1 = 0.5$ Pa \cdot s) of initial thickness of $T_0 = 25$ nm per layer and $R = 2$ cm as they approach each other in air at a terminal driving velocity of $V = 0.3$ nm/s. A jump of $D_j \approx 200$ nm occurred at time $t = 150$ sec (time in arbitrary units) when the mica substrate surfaces were ~ 250 nm apart. When coalescence occurs, the FEKO fringe pattern changes in a similar way to that recently shown in Ref. [10]. (b),(c) Two PBD films of viscosity $\mu_1 = 33.6$ Pa \cdot s approaching each other in PDMS of viscosity $\mu_2 = 0.5$ Pa \cdot s where the initial film thicknesses were $T_0 = 120$ nm and 25 nm in (b) and (c), respectively. In all the cases studied, at low approach velocities V , just prior to coalescence, the films thickened (bulged out) at the center but thinned around the center, as shown in the two schematic insets.

deformations of 10–20 nm would still be much smaller than the droplet radii (of 1–10 μ m). However, for even smaller droplets the droplet volume may no longer act as an infinite reservoir of liquid, which is assumed in Eq. (1).

We end by stressing the quasistatic, near-equilibrium nature of our system and observations, which is relevant

to low approach rates. As shown here, such systems appear to be amenable to quantitative theoretical analysis. In contrast, as illustrated schematically in Fig. 2(b), the deformations and coalescence mechanisms at high approach rates, which also involve viscous (hydrodynamic) forces, can be quite different (for example, the bulging can be in the opposite direction) and very much more complex than under the quasistatic conditions of Fig. 2(a). Quantitative experiments on such systems are currently in progress.

This work was supported by NASA Grant No. NAG3-2115. We thank Nobuo Maeda and Gary Leal for helpful discussions and suggestions.

*Now at Department of Chemical Engineering and Materials Science, University of California, Davis, CA 95616, USA.

†Now at Department of Chemical Engineering, Lamar University, Beaumont, TX 77710-0053, USA.

‡Corresponding author.

Electronic address: jacob@engineering.ucsb.edu

- [1] D. Katoshevski, A. Nenes, and J. H. Seinfeld, *J. Aerosol Sci.* **30**, 503 (1999).
- [2] J. C. Lasheras and E. J. Hopfinger, *Annu. Rev. Fluid Mech.* **32**, 275 (2000).
- [3] D. Rosenfeld, *Science* **287**, 1793 (2000).
- [4] J. H. Seinfeld, *Air Pollution: Physical and Chemical Fundamentals* (McGraw-Hill, New York, 1975).
- [5] A. K. Chesters, *Chem. Eng. Res. Des.* **69**, 259 (1991).
- [6] A. B. Metzner, J. L. White, and M. M. Denn, *AIChE J.* **12**, 863 (1966).
- [7] Lord Rayleigh, *Proc. London Math. Soc.* **10**, 4 (1879).
- [8] B. V. Derjaguin and N. V. Churaev, *J. Colloid Interface Sci.* **54**, 157 (1976).
- [9] H. K. Christenson, *Phys. Rev. Lett.* **73**, 1821 (1994).
- [10] N. Maeda, J. N. Israelachvili, and M. M. Kohonen, *Proc. Natl. Acad. Sci. U.S.A.* **100**, 803 (2003).
- [11] J. N. Israelachvili, *Intermolecular & Surface Forces* (Academic Press, London, 1991).
- [12] J. N. Israelachvili and P. M. McGuiggan, *J. Mater. Res.* **5**, 2223 (1990).
- [13] J. N. Israelachvili, *J. Colloid Interface Sci.* **44**, 259 (1973).
- [14] J. N. Israelachvili and G. E. Adams, *J. Chem. Soc. Faraday Trans. 1* **74**, 975 (1978).
- [15] H. Yang *et al.*, *Phys. Fluids* **13**, 1087 (2001).
- [16] R. G. Horn and J. N. Israelachvili, *J. Chem. Phys.* **75**, 1400 (1981).
- [17] M. L. Forcada, M. M. Jakas, and A. Grasmarti, *J. Chem. Phys.* **95**, 706 (1991).
- [18] D. Bhatt, J. Newman, and C. J. Radke, *Langmuir* **17**, 116 (2001).
- [19] D. Y. C. Chan, R. R. Dagastine, and L. R. White, *J. Colloid Interface Sci.* **236**, 141 (2001).
- [20] P. Attard and S. J. Miklavcic, *Langmuir* **17**, 8217 (2001).
- [21] P. Attard and S. J. Miklavcic, *J. Colloid Interface Sci.* **247**, 255 (2002).
- [22] S. J. Miklavcic and P. Attard, *J. Phys. A* **34**, 7849 (2001).